

Theory for the solvation of nonpolar solutes in water

T. Urbic and V. Vlachy

Faculty of Chemistry and Chemical Technology, University of Ljubljana, Aškerčeva 5, 1000 Ljubljana, Slovenia

Yu. V. Kalyuzhnyi

Institute for Condensed Matter Physics, Svientsitskoho 1, 79011 Lviv, Ukraine

K. A. Dill

Department of Pharmaceutical Chemistry, University of California, San Francisco, California 94143-1204, USA

(Received 16 July 2007; accepted 13 August 2007; published online 5 November 2007)

We recently developed an angle-dependent Wertheim integral equation theory (IET) of the Mercedes-Benz (MB) model of pure water [Silverstein *et al.*, *J. Am. Chem. Soc.* **120**, 3166 (1998)]. Our approach treats explicitly the coupled orientational constraints within water molecules. The analytical theory offers the advantage of being less computationally expensive than Monte Carlo simulations by two orders of magnitude. Here we apply the angle-dependent IET to studying the hydrophobic effect, the transfer of a nonpolar solute into MB water. We find that the theory reproduces the Monte Carlo results qualitatively for cold water and quantitatively for hot water.

© 2007 American Institute of Physics. [DOI: [10.1063/1.2779329](https://doi.org/10.1063/1.2779329)]

I. INTRODUCTION

Understanding solute-solvent interactions in aqueous solutions is important for biology and chemistry. Several important reviews have been published on this subject.^{1–10} Theoretical models of various degrees of sophistication have been developed to capture the anomalous properties of water and of aqueous solutions (for review, see Refs. 11 and 12).

The principal challenge in modeling the physics of water comes from the orientation-dependent hydrogen bonding interactions, particularly from the strong coupling between different hydrogen bonding arms within a given water molecule. Much of liquid theory is applicable either to molecules, such as argon, for which the interactions are centrosymmetric, or to dipolar fluids, which have simple uncoupled orientation-dependent interactions. It has been much more challenging to develop analytical ways to treat coupled orientational interactions in liquids. In order to have a workbench to develop theory for such situations, it is useful to have a model having the same orientational physics problems that real water was, and yet is simplified enough to be well understood through, say, Monte Carlo computer simulations. The simplified model that is of interest here is the Mercedes-Benz model. The Mercedes-Benz (MB) model¹³ is one of the simplest and best-understood models of water.^{14–20} MB molecules are two-dimensional Lennard-Jones disks having three hydrogen bonding (HB) arms, arranged as in the Mercedes-Benz logo. Constant-pressure Monte Carlo simulations have shown that this simple model predicts qualitatively the density anomaly, the minimum in the isothermal compressibility as a function of temperature, the large heat capacity, and the experimental trends for the thermodynamic properties of solvation of nonpolar solutes.¹⁵

Here, we describe a more analytical approach to nonpolar solvation in water. We have previously studied the MB model of pure water by two different analytical approaches: (1) averaging over orientations (which we call the orientationally averaged approach) and (2) where orientations are treated explicitly. In particular, in previous work^{21–23} Wertheim's theory for associating fluids^{24,25} was applied to the MB model of water through a thermodynamic perturbation theory^{24,25} (TPT) and an integral equation theory (IET).^{23,24,26} We found that both of these analytical approaches, using an orientational averaging approximation, are in semiquantitative agreement with the Monte Carlo simulation results for the temperature dependence of the molar volume, isothermal compressibility, thermal expansion coefficient, and heat capacity. IET also correctly predicts the pair correlation functions of MB model water. However, in general, we found that the orientationally averaged treatment of the Ornstein-Zernike equation tends, not surprisingly, to be most accurate for high temperatures and less accurate for cold water, where water structuring from hydrogen bonding is stronger.

More recently, to overcome those limitations, we have also developed a treatment based on an Ornstein-Zernike equation that can explicitly handle the orientations of one molecule relative to another.²³ This orientationally specific theory is based on the expansion of the two-particle correlation functions in a complete set of orthogonal functions.^{27–32} It performs better than the orientationally averaged theory for pure water. Here, we apply this orientationally specific treatment to nonpolar solvation. One advantage of these IET approaches to water, both in the pure state and as a solvent, is that it is about two orders of magnitude faster than brute force Monte Carlo simulations.

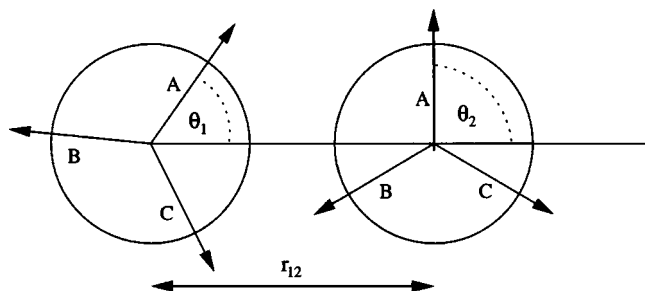


FIG. 1. The MB model of water. Two MB water molecules separated by a distance r_{12} . The angles that the molecules make with the intermolecular axis are θ_1 and θ_2 .

II. THE MODEL

We consider here a mixture of two-dimensional MB water molecules with nonpolar solutes. The nonpolar solute molecules were modeled as Lennard-Jones disks with no hydrogen bonding arms. Each MB water molecule is represented as a two-dimensional Lennard-Jones disk with three arms separated by an angle of 120° (see Fig. 1).¹⁵ The interaction potential between two MB particles is a sum of a Lennard-Jones term and a HB term,

$$U(\mathbf{X}_i, \mathbf{X}_j) = U_{\text{LJ}}^{11}(r_{ij}) + U_{\text{HB}}(\mathbf{X}_i, \mathbf{X}_j), \quad (1)$$

where r_{ij} is the distance between centers of particles i and j and \mathbf{X}_i denotes the vector representing the coordinates and the orientation of the i th particle.

$$U_{\text{LJ}}^{ij}(r_{ij}) = 4\varepsilon_{\text{LJ}}^{ij} \left(\left(\frac{\sigma_{\text{LJ}}^{ij}}{r_{ij}} \right)^{12} - \left(\frac{\sigma_{\text{LJ}}^{ij}}{r_{ij}} \right)^6 \right), \quad (2)$$

where $\varepsilon_{\text{LJ}}^{ij}$ is the well depth and σ_{LJ}^{ij} is the contact parameter between i^{th} and j^{th} particles. The hydrogen bonding part of the interaction potential is

$$U_{\text{HB}}(\mathbf{X}_i, \mathbf{X}_j) = \sum_{k,l=1}^3 U_{\text{HB}}^{kl}(r_{ij}, \theta_1, \theta_2), \quad (3)$$

where U_{HB}^{kl} describes the interaction between two arms of different molecules,

$$U_{\text{HB}}^{kl}(r_{ij}, \theta_1, \theta_2) = \varepsilon_{\text{HB}} G(r_{ij} - r_{\text{HB}}) G(\mathbf{i}_k \mathbf{u}_{ij} - 1) G(\mathbf{j}_l \mathbf{u}_{ij} + 1). \quad (4)$$

Expressing the scalar products explicitly gives the following form of the HB potential:

$$U_{\text{HB}}^{kl}(r_{ij}, \theta_i, \theta_j) = \varepsilon_{\text{HB}} G(r_{ij} - r_{\text{HB}}) G(\cos(\theta_i + (2\pi/3)(k-1)) - 1) \times G(\cos(\theta_j + (2\pi/3)(l-1)) + 1), \quad (5)$$

where k and l index the different arms ($A=1$, $B=2$, and $C=3$) and $G(x)$ is an unnormalized Gaussian function,

$$G(x) = \exp\left(-\frac{x^2}{2\sigma^2}\right). \quad (6)$$

Further, $\varepsilon_{\text{HB}} = -1$ is an energy parameter and $r_{\text{HB}} = 1$ is a characteristic hydrogen bond length. \mathbf{u}_{ij} is the unit vector along \mathbf{r}_{ij} and \mathbf{i}_k is the unit vector representing the k^{th} arm of the i^{th}

particle, where θ_i is the orientation of i^{th} particle, as shown in Fig. 1. The strongest hydrogen bond occurs when an arm of one particle is collinear with the arm of another particle and when the two arms point in opposite directions. The water-water Lennard-Jones (LJ) well depth $\varepsilon_{\text{LJ}}^{11}$ is one-tenth of HB interaction energy ε_{HB} and the Lennard-Jones contact parameter σ_{LJ}^{11} is $0.7r_{\text{HB}}$. Since the three hydrogen bonding arms of one particular MB molecule are labeled A, B, and C, that molecule can be in any one of eight different states: i.e., it can have zero hydrogen bonds with other molecules, or a single hydrogen bond, A-, B-, C-, two hydrogen bonds, AB-, AC-, BC-, or it can have all three hydrogen bonds, ABC-.

The nonpolar solutes are modeled as Lennard-Jones disks without hydrogen bonding arms. In a recent Monte Carlo study of the MB hydrophobic effect,¹⁷ the solution was taken to be infinitely dilute so that only the solvent-solute interactions were specified. In the present IET and TPT calculations, we explored low but finite concentrations of solute in water. The solute-solute interaction is described by Eq. (2). The standard Lorentz-Berthelot rules³³ were assumed in calculating the solute-water and solute-solute interactions as the solute size parameter σ_{LJ}^{22} changed from $0.1r_{\text{HB}}$ to $4.0r_{\text{HB}}$. The LJ well depth $\varepsilon_{\text{LJ}}^{ij}$ was the same for all interaction pairs and as above equal to one-tenth of HB interaction energy ε_{HB} .

III. THEORY

In this section we extend the orientation-dependent version of Wertheim's multidensity Ornstein-Zernike (OZ) equation introduced in our previous paper²³ to describe a mixture of MB water and nonpolar solute molecules. We present a multidensity theory suitable for a two-dimensional mixture of molecules with multiple bonding arms and molecules without bonding sites.

A. Orientation-dependent OZ equation

We define the center of particle 1 as the origin of the coordinate system and the center of particle 2 is separated from the center of 1 by a distance r_{12} . The angles θ_i are measured with respect to the intermolecular axis (see Fig. 1). We expand the correlation functions in a complete set of orthogonal functions.^{23,29,30} We expand $z_{\alpha\beta}$ as

$$z_{\alpha\beta}(r, \theta_1, \theta_2) = \sum_{m,j=-L}^L z_{\alpha\beta}(r, m, j) \exp[i(m\theta_1 + j\theta_2)]. \quad (7)$$

While the summation in this expression formally extends from minus to plus infinity ($L \rightarrow \infty$), in most cases only a small number of coefficients is needed (typically L is less than 9) for a good representation of the fluid structure and thermodynamics. The expansion coefficients in k space $\hat{z}(k, m, j)$ are linked to $z(r, m, j)$ by the relation

$$\hat{z}_{\alpha\beta}(k, m, j) = 2\pi i^{m+j} \int_0^\infty z_{\alpha\beta}(r, m, j) J_{m+j}(kr) r dr, \quad (8)$$

where J_p denotes the p^{th} order Bessel function of the first kind. The Ornstein-Zernike equation can be written in matrix form as²³

$$\hat{\mathbf{h}} = \hat{\mathbf{c}} + \hat{\mathbf{c}}^{-1} \hat{\boldsymbol{\rho}} \hat{\mathbf{h}}. \quad (9)$$

Finally, it is convenient to write Eq. (9) in terms of function $\hat{\mathbf{t}} = \hat{\mathbf{h}} - \hat{\mathbf{c}}$ as

$$\hat{\mathbf{t}} = (\mathbf{I} - \hat{\mathbf{c}}^{-1} \hat{\boldsymbol{\rho}})^{-1} \hat{\mathbf{c}}^{-1} \hat{\boldsymbol{\rho}} \hat{\mathbf{c}}. \quad (10)$$

$\hat{\mathbf{t}}$, $\hat{\mathbf{h}}$, and $\hat{\mathbf{c}}$ are matrices of the form

$$\hat{\mathbf{z}} = \begin{pmatrix} \hat{\mathbf{z}}_{0,0}^{11} & \hat{\mathbf{z}}_{0,A}^{11} & \hat{\mathbf{z}}_{0,B} & \hat{\mathbf{z}}_{0,C}^{11} & \hat{\mathbf{z}}_{0,AB}^{11} & \hat{\mathbf{z}}_{0,AC} & \hat{\mathbf{z}}_{0,BC}^{11} & \hat{\mathbf{z}}_{0,ABC}^{11} & \hat{\mathbf{z}}_0^{12} \\ \hat{\mathbf{z}}_{A,0}^{11} & \hat{\mathbf{z}}_{A,A}^{11} & \hat{\mathbf{z}}_{A,B} & \hat{\mathbf{z}}_{A,C}^{11} & \hat{\mathbf{z}}_{A,AB}^{11} & \hat{\mathbf{z}}_{A,AC} & \hat{\mathbf{z}}_{A,BC}^{11} & \hat{\mathbf{z}}_{A,ABC}^{11} & \hat{\mathbf{z}}_A^{12} \\ \hat{\mathbf{z}}_{B,0}^{11} & \hat{\mathbf{z}}_{B,A}^{11} & \hat{\mathbf{z}}_{B,B} & \hat{\mathbf{z}}_{B,C}^{11} & \hat{\mathbf{z}}_{B,AB}^{11} & \hat{\mathbf{z}}_{B,AC} & \hat{\mathbf{z}}_{B,BC}^{11} & \hat{\mathbf{z}}_{B,ABC}^{11} & \hat{\mathbf{z}}_B^{12} \\ \hat{\mathbf{z}}_{C,0}^{11} & \hat{\mathbf{z}}_{C,A}^{11} & \hat{\mathbf{z}}_{C,B} & \hat{\mathbf{z}}_{C,C}^{11} & \hat{\mathbf{z}}_{C,AB}^{11} & \hat{\mathbf{z}}_{C,AC} & \hat{\mathbf{z}}_{C,BC}^{11} & \hat{\mathbf{z}}_{C,ABC}^{11} & \hat{\mathbf{z}}_C^{12} \\ \hat{\mathbf{z}}_{AB,0}^{11} & \hat{\mathbf{z}}_{AB,A}^{11} & \hat{\mathbf{z}}_{AB,B} & \hat{\mathbf{z}}_{AB,C}^{11} & \hat{\mathbf{z}}_{AB,AB}^{11} & \hat{\mathbf{z}}_{AB,AC} & \hat{\mathbf{z}}_{AB,BC}^{11} & \hat{\mathbf{z}}_{AB,ABC}^{11} & \hat{\mathbf{z}}_{AB}^{12} \\ \hat{\mathbf{z}}_{AC,0}^{11} & \hat{\mathbf{z}}_{AC,A} & \hat{\mathbf{z}}_{AC,B} & \hat{\mathbf{z}}_{AC,C}^{11} & \hat{\mathbf{z}}_{AC,AB}^{11} & \hat{\mathbf{z}}_{AC,AC} & \hat{\mathbf{z}}_{AC,BC} & \hat{\mathbf{z}}_{AC,ABC}^{11} & \hat{\mathbf{z}}_{AC}^{12} \\ \hat{\mathbf{z}}_{BC,0}^{11} & \hat{\mathbf{z}}_{BC,A} & \hat{\mathbf{z}}_{BC,B} & \hat{\mathbf{z}}_{BC,C}^{11} & \hat{\mathbf{z}}_{BC,AB}^{11} & \hat{\mathbf{z}}_{BC,AC} & \hat{\mathbf{z}}_{BC,BC}^{11} & \hat{\mathbf{z}}_{BC,ABC}^{11} & \hat{\mathbf{z}}_{BC}^{12} \\ \hat{\mathbf{z}}_{ABC,0} & \hat{\mathbf{z}}_{ABC,A} & \hat{\mathbf{z}}_{ABC,B} & \hat{\mathbf{z}}_{ABC,C}^{11} & \hat{\mathbf{z}}_{ABC,AB}^{11} & \hat{\mathbf{z}}_{ABC,AC} & \hat{\mathbf{z}}_{ABC,BC}^{11} & \hat{\mathbf{z}}_{ABC,ABC}^{11} & \hat{\mathbf{z}}_{ABC}^{12} \\ \hat{\mathbf{z}}_0^{21} & \hat{\mathbf{z}}_A^{21} & \hat{\mathbf{z}}_B^{21} & \hat{\mathbf{z}}_C^{21} & \hat{\mathbf{z}}_{AB}^{21} & \hat{\mathbf{z}}_{AC}^{21} & \hat{\mathbf{z}}_{BC}^{21} & \hat{\mathbf{z}}_{ABC}^{21} & \hat{\mathbf{z}}^{22} \end{pmatrix}. \quad (11)$$

In this expression, $\hat{\mathbf{z}}_{\alpha,\beta}^{11}$, $\hat{\mathbf{z}}_{\alpha}^{12}$, $\hat{\mathbf{z}}_{\alpha}^{21}$, and $\hat{\mathbf{z}}^{22}$ are matrices of dimensionality $(2L+1) \times (2L+1)$ defined as $\hat{\mathbf{z}}(m, j) = \hat{z}(k, m, j)$. $\hat{\mathbf{c}}^{-1}$ is matrix of the same dimensionality defined as $\hat{c}^{-}(k, m, p) = \hat{c}(k, m, -p)$ and $\boldsymbol{\rho}$ is the matrix of partial densities,

$$\boldsymbol{\rho} = \begin{pmatrix} \rho_1 \mathbf{I} & \rho_1 \mathbf{I} & \rho_1 \mathbf{I} & \rho_1 \mathbf{I} & \rho_1 \mathbf{I} & \rho_1 \mathbf{I} & \rho_1 \mathbf{I} & \rho_1 \mathbf{I} & 0 \\ \rho_1 \mathbf{I} & 0 & (\rho_1 x_2 / x_1^2) \mathbf{I} & (\rho_1 x_2 / x_1^2) \mathbf{I} & 0 & 0 & (\rho_1 x_3 / x_1 x_2) \mathbf{I} & 0 & 0 \\ \rho_1 \mathbf{I} & (\rho_1 x_2 / x_1^2) \mathbf{I} & 0 & (\rho_1 x_2 / x_1^2) \mathbf{I} & 0 & (\rho_1 x_3 / x_1 x_2) \mathbf{I} & 0 & 0 & 0 \\ \rho_1 \mathbf{I} & (\rho_1 x_2 / x_1^2) \mathbf{I} & (\rho_1 x_2 / x_1^2) \mathbf{I} & 0 & (\rho_1 x_3 / x_1 x_2) \mathbf{I} & 0 & 0 & 0 & 0 \\ \rho_1 \mathbf{I} & 0 & 0 & (\rho_1 x_3 / x_1 x_2) \mathbf{I} & 0 & 0 & 0 & 0 & 0 \\ \rho_1 \mathbf{I} & 0 & (\rho_1 x_3 / x_1 x_2) \mathbf{I} & 0 & 0 & 0 & 0 & 0 & 0 \\ \rho_1 \mathbf{I} & (\rho_1 x_3 / x_1 x_2) \mathbf{I} & 0 & 0 & 0 & 0 & 0 & 0 & 0 \\ \rho_1 \mathbf{I} & 0 & 0 & 0 & 0 & 0 & 0 & 0 & 0 \\ 0 & 0 & 0 & 0 & 0 & 0 & 0 & 0 & \rho_2 \mathbf{I} \end{pmatrix}, \quad (12)$$

where \mathbf{I} denotes the identity matrix, ρ_1 is the density of MB water, and ρ_2 is the density of the solute molecules. The physical meaning of the partial densities x_i of the bonding sites is as follows: x_1 is the fraction of nonbonded particles at one particular arm (arm A, for example), x_2 is the fraction of nonbonded particles for two selected arms (arms B and C, for example), and x_3 is the fraction of particles not bonded to any arm. They are calculated by procedures described in our previous paper.²³ The integral equation described above contains two unknown correlation functions (h and c). A closure condition, i.e., an additional relation between the h and c functions, is required (see, for example, Ref. 33) to solve the integral equation.

B. Closure relations

Here, for the closure relations for coefficients $c_{\alpha,\beta}^{11}(r, m, j)$, $c_{\alpha}^{12}(r, m, j)$, $c_{\alpha}^{21}(r, m, j)$, and $c^{22}(r, m, j)$ we used the polymer soft mean-spherical approximation (PSMSA).²³

In this closure we divide the LJ potential into a short-range reference part $U_0^{ij}(r)$ and a longer-range perturbation part $U_1^{ij}(r)$ as suggested elsewhere,³⁴

$$U_{\text{LJ}}^{ij}(r) = U_0^{ij}(r) + U_1^{ij}(r), \quad (13)$$

where

$$U_0^{ij}(r) = \begin{cases} U_{\text{LJ}}^{ij}(r) + \varepsilon_{\text{LJ}}^{ij} & r \geq r_m^{ij} \\ 0 & r < r_m^{ij} \end{cases}$$

and

$$U_1^{ij}(r) = \begin{cases} -\varepsilon_{\text{LJ}}^{ij} & r \geq r_m^{ij} \\ U_{\text{LJ}}^{ij}(r) & r < r_m^{ij} \end{cases}.$$

The distance r_m^{ij} that separates these two components is chosen to be the position of a minimum of the LJ part of the potential function, i.e., $r_m^{ij} = 2^{1/6} \sigma_{\text{LJ}}^{ij}$. We also define $f_0^{ij}(r)$ and $e_{\text{LJ}}^{ij}(r)$ as

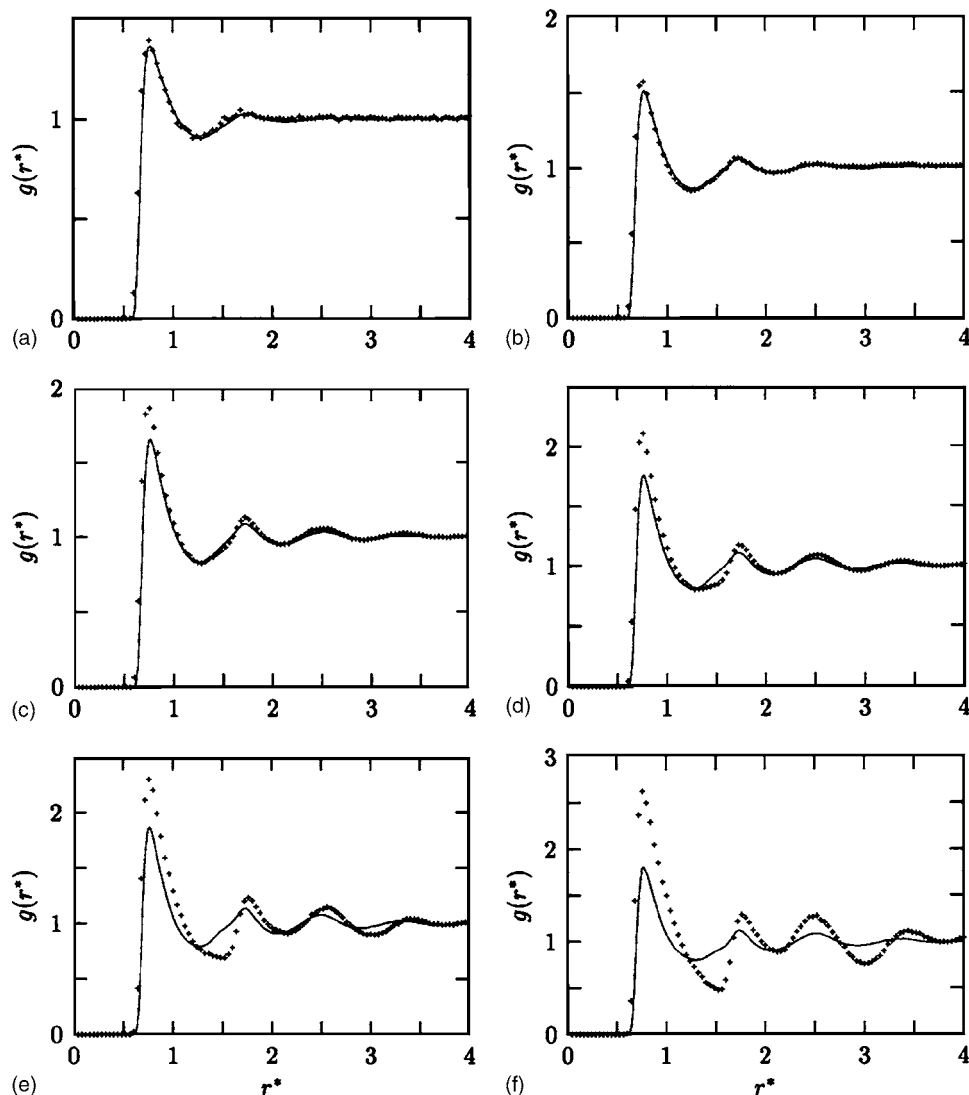


FIG. 2. The solute-water pair distribution function $g(r^*)$ at different temperatures. Top left is the hottest water; bottom right is the coldest water. The Monte Carlo result (Ref. 36) is presented by symbols and the IET result by a solid line. Distribution functions are presented for state points (a) $T^* = 0.36$, $\rho_1^* = 0.534$, (b) $T^* = 0.28$, $\rho_1^* = 0.741$, (c) $T^* = 0.24$, $\rho_1^* = 0.870$, (d) $T^* = 0.21$, $\rho_1^* = 0.943$, (e) $T^* = 0.18$, $\rho_1^* = 0.990$, and (f) $T^* = 0.16$, $\rho_1^* = 0.900$. The ratio of the density of water to the density of nonpolar molecules is 60:1. The LJ parameter for nonpolar molecules is $\sigma_{\text{LJ}}^{22} = 0.7r_{\text{HB}}$.

$$f_0^{ij}(r) = \exp\left[-\frac{U_0^{ij}(r)}{k_B T}\right] - 1, \quad (14)$$

$$e_{\text{LJ}}^{ij}(r) = \exp\left[-\frac{U_{\text{LJ}}^{ij}(r)}{k_B T}\right]. \quad (15)$$

The water-water PSMSA closure relations²³ can be written as

$$\begin{aligned} c_{\alpha,\beta}^{11}(r,m,j) &= f_0^{11}(r)y_{\alpha,\beta}^{11}(r,m,j) \\ &+ e_{\text{LJ}}^{11}(r) \sum_{D \in \alpha} \sum_{E \in \beta} \sum_{p,q=-L}^L \frac{\sigma_{ABC-\alpha} \sigma_{ABC-\beta}}{\sigma_{ABC-\alpha+D} \sigma_{ABC-\beta+E}} \\ &\times f_{DE}(r, -p+m, -q+j) y_{\alpha-D, \beta-E}^{11}(r,p,q) (1 - \delta_{\alpha,0}) \\ &\times (1 - \delta_{\beta,0}). \end{aligned} \quad (16)$$

$\delta_{\alpha,0}$ is the delta function and $\sigma_{\mu\nu}$ are Wertheim's density parameters.^{23,24} $c_{0,0}^{11}(r,m,j)$ has the following special form:

$$c_{0,0}^{11}(r,m,j) = f_0^{11}(r)y_{0,0}^{11}(r,m,j) - (f_0^{11}(r) + 1) \frac{U_1^{11}(r)}{k_B T}. \quad (17)$$

Water-solute closures are

$$c_0^{12}(r,m,j) = f_0^{12}(r)y_0^{12}(r,m,j) - (f_0^{12}(r) + 1) \frac{U_1^{12}(r)}{k_B T}, \quad (18)$$

$$c_\alpha^{12}(r,m,j) = f_0^{12}(r)y_\alpha^{12}(r,m,j), \quad (19)$$

$$c_0^{21}(r,m,j) = f_0^{21}(r)y_0^{21}(r,m,j) - (f_0^{21}(r) + 1) \frac{U_1^{21}(r)}{k_B T}, \quad (20)$$

$$c_\alpha^{21}(r,m,j) = f_0^{21}(r)y_\alpha^{21}(r,m,j), \quad (21)$$

and solute-solute closure,

$$c_0^{22}(r,m,j) = f_0^{22}(r)y_0^{22}(r,m,j) - (f_0^{22}(r) + 1) \frac{U_1^{22}(r)}{k_B T}. \quad (22)$$

We solved the OZ equation [Eq. (10)] along with the closure conditions by using a direct iteration method. We performed the forward and inverse Bessel-Fourier transforms—which are needed to couple the correlation functions in real and Fourier spaces—by using the method of Talman.³⁵ This method gives an efficient way to sample both the rapidly varying part of the correlation functions at small distances and the long-ranged part, using a relatively small number of grid points, $n=512$.

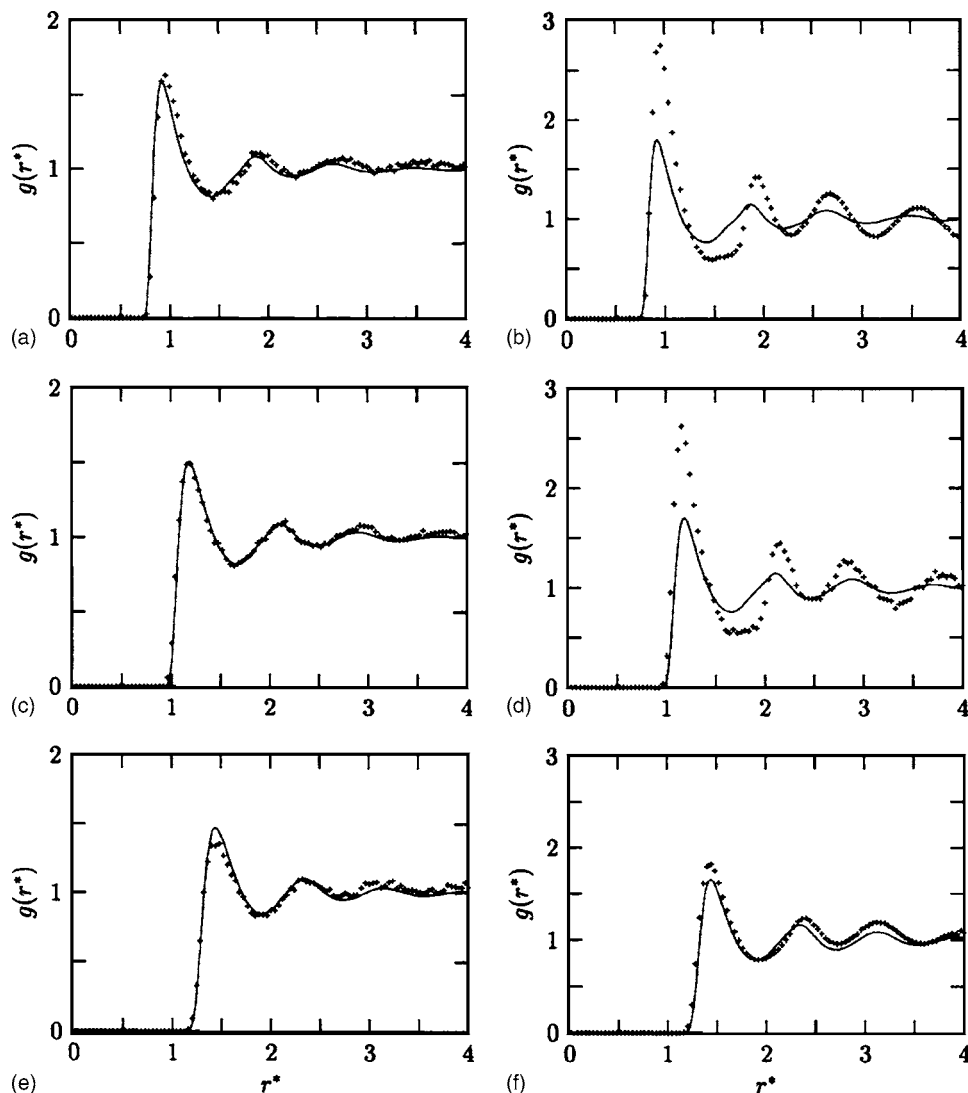


FIG. 3. Solute-water pair distribution function $g(r^*)$ at different temperatures and sizes of nonpolar solute. The Monte Carlo result (Ref. 36) is presented by symbols and the IET result by solid line. Distribution functions are presented for the following state points and sizes of nonpolar molecules (a) $\sigma_{LJ}^{22} = 1.0 r_{HB}$, $T^* = 0.24$, $\rho_1^* = 0.870$, (b) $\sigma_{LJ}^{22} = 1.0 r_{HB}$, $T^* = 0.18$, $\rho_1^* = 0.990$, (c) $\sigma_{LJ}^{22} = 1.5 r_{HB}$, $T^* = 0.24$, $\rho_1^* = 0.870$, (d) $\sigma_{LJ}^{22} = 1.5 r_{HB}$, $T^* = 0.18$, $\rho_1^* = 0.990$, (e) $\sigma_{LJ}^{22} = 2.0 r_{HB}$, $T^* = 0.24$, $\rho_1^* = 0.870$, and (f) $\sigma_{LJ}^{22} = 2.0 r_{HB}$, $T^* = 0.18$, $\rho_1^* = 0.990$. The ratio of the density of water to the density of nonpolar molecules is 60:1.

The (0,0) harmonics of the partial correlation functions are summed to give orientationally averaged total correlation function,

$$g^{11}(r) = \sum_{\alpha,\beta} h_{\alpha,\beta}^{11}(r,0,0) + 1, \quad (23)$$

$$g^{12}(r) = \sum_{\alpha} h_{\alpha}^{12}(r,0,0) + 1, \quad (24)$$

$$g^{22}(r) = h^{22}(r,0,0) + 1, \quad (25)$$

where α and β again are the bonding states of a MB molecule. Similar expressions are used to get the higher coefficients of the total pair correlation function,

$$g^{11}(r,m,j) = \sum_{\alpha,\beta} (h_{\alpha,\beta}^{11}(r,m,j) + \delta_{\alpha,0}\delta_{\beta,0}\delta_{m,0}\delta_{j,0}). \quad (26)$$

The two-particle distribution function $g(r, \theta_1, \theta_2)$ can now be calculated as

$$g^{11}(r, \theta_1, \theta_2) = \sum_{m,j=-L}^L g^{11}(r,m,j) \exp[i(m\theta_1 + j\theta_2)]. \quad (27)$$

For the present study of nonpolar solvation, we have used the same MB model parameters that we previously used for studying pure MB water.^{15,23} $\epsilon_{HB} = -1$, $r_{HB} = 1$, $\epsilon_{LJ} = 0.1\epsilon_{HB}$, and $\sigma_{LJ}^{11} = 0.7r_{HB}$. All the results are shown in reduced units: the excess internal energy and temperature are normalized to the HB energy parameter ϵ_{HB} ($A^* = A/|\epsilon_{HB}|$, $T^* = k_B T/|\epsilon_{HB}|$) and the distances are scaled to the hydrogen bond characteristic length r_{HB} ($r^* = r/r_{HB}$).

IV. RESULTS AND DISCUSSION

The results for solute-water pair distribution functions for different temperatures are shown in Fig. 2. The Monte Carlo results are presented by symbols and the results provided by angle-dependent IET with PSMSA closure by solid line. The size of nonpolar solute molecule is the same as the size of water: $\sigma_{LJ}^{22} = 0.7r_{HB}$, and the ratio between water density and density of nonpolar solute is 60:1.

Figure 2 shows that angle-dependent IET (ADIET) gives better agreement with the Monte Carlo results than the orientationally averaged version of IET. ADIET more correctly predicts the r dependence of the maxima and minima of the pair distribution functions, but it fails to predict correct

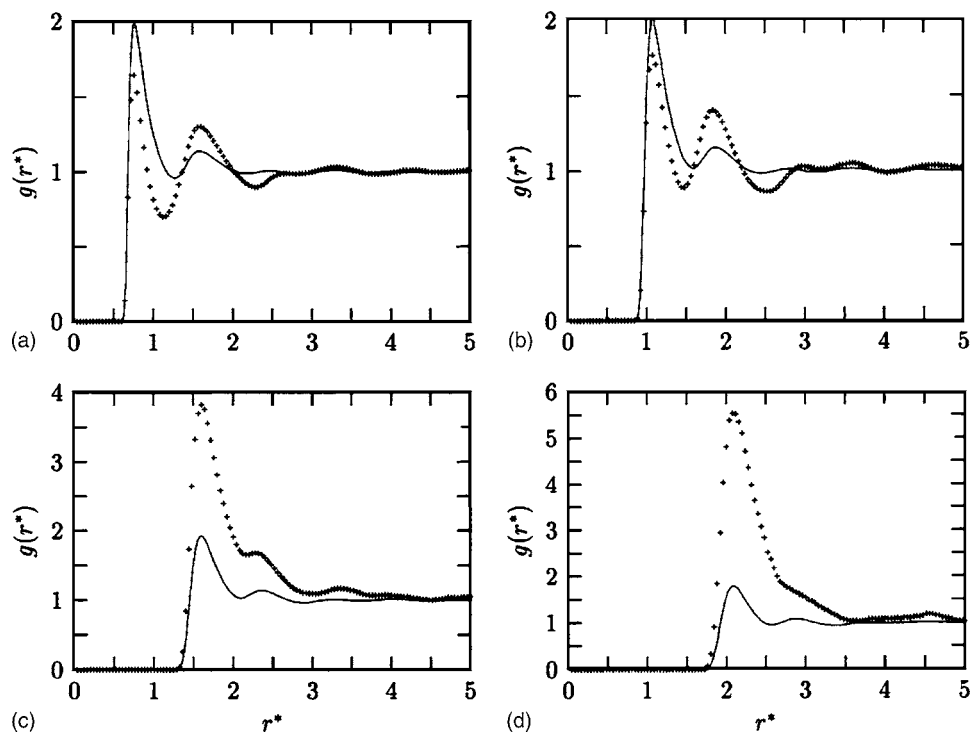


FIG. 4. Solute-solute pair distribution function $g(r^*)$ at different temperatures and solute sizes. The Monte Carlo result is presented by symbols and the IET result by a solid line. Distribution functions are presented for the following sizes of nonpolar molecules: (a) $\sigma_{\text{LJ}}^{22}=0.7r_{\text{HB}}$, (b) $\sigma_{\text{LJ}}^{22}=1.0r_{\text{HB}}$, (c) $\sigma_{\text{LJ}}^{22}=1.5r_{\text{HB}}$, and (d) $\sigma_{\text{LJ}}^{22}=2.0r_{\text{HB}}$. Temperature of the solution is $T^*=0.21$ and density of water $\rho_1^*=0.943$. The ratio of the density of water to the density of nonpolar molecules is 60:1.

heights of them. The ADIET appears to underestimate the internal rigidity in water molecule structures.

Figure 3 shows how the radius of the solute affects the solute-water interactions. Previous Monte Carlo simulations of the MB model¹⁷ showed that if a solute molecule is as small as a water molecule, it causes first-shell waters to become orientationally ordered to avoid wasting hydrogen bonds. In contrast, around large solute molecules, water molecules are sterically forced to waste hydrogen bonds. Our present IET results are consistent with this picture and are in good agreement with simulation results for all solute sizes at

higher temperatures. At lower temperatures, however, agreement is good only for solutes larger than $r^*=1.5$. For molecules smaller than $r^*=1.5$ IET fails to predict the correct heights of the peaks. As we also found in our earlier work on pure water, these limitations of the IET theory are greatest in situations involving high degrees of hydrogen-bonded water structuring. Smaller molecules insert into cavities formed by water molecules while bigger molecules must break water structure when they are solvated in water. Figure 4 shows solute-solute pair distribution functions for different sizes of nonpolar solutes. While we find that treating the orientations

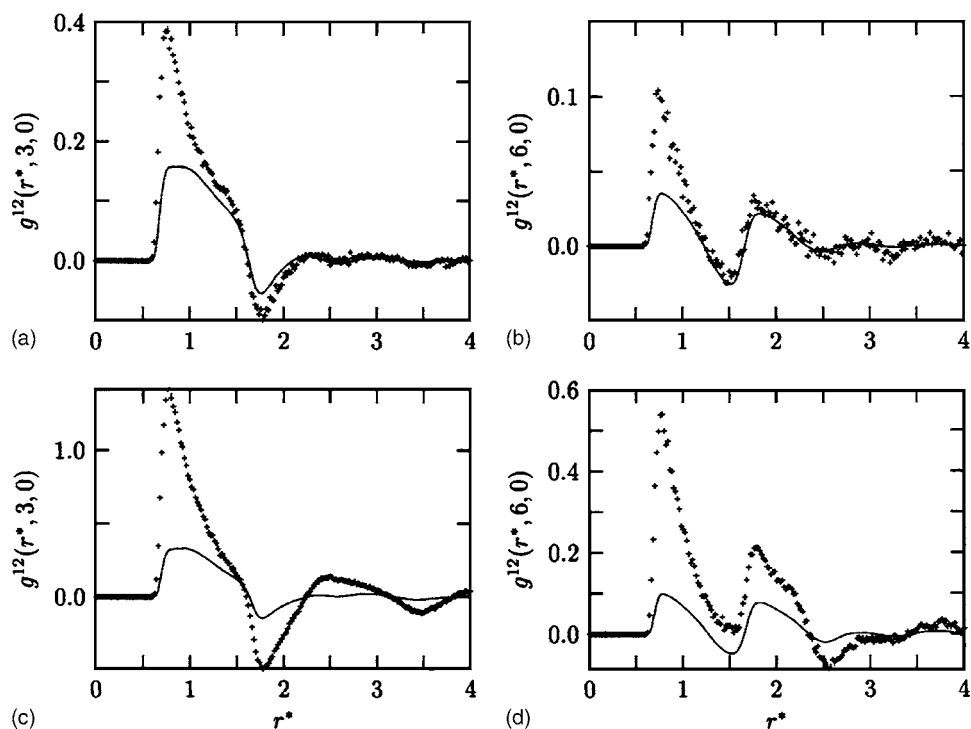


FIG. 5. The coefficients of the expansion of the two-particle solute-water distribution function at [(a) and (b)] $T^*=0.28$ and [(c) and (d)] $T^*=0.18$. Density of the water is $\rho_1^*=0.9$ and ratio between density of water and nonpolar molecules is 60:1. The Monte Carlo result is presented by symbols and the IET result by solid line. LJ parameter for nonpolar molecules is $\sigma_{\text{LJ}}^{22}=0.7r_{\text{HB}}$.

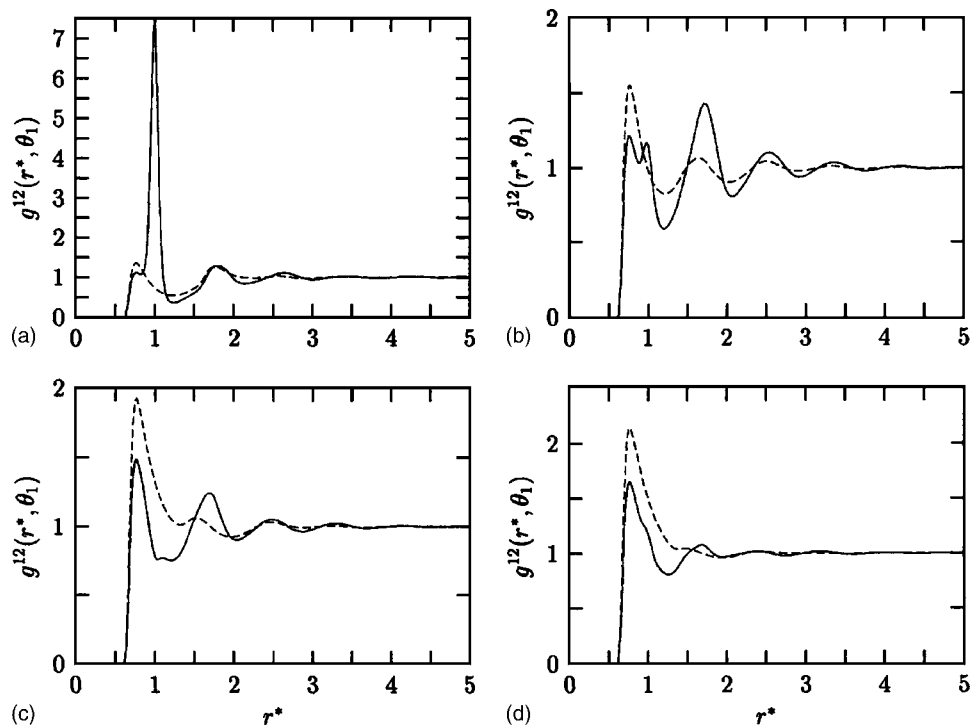


FIG. 6. Water-water pair distribution, $g(r^*, \theta_1)$ for various orientations θ_1 of the water molecule, averaged over all possible θ_2 values at $T^* = 0.24$, density of water $\rho_1^* = 0.87$ and ratio between number of molecules of water and nonpolar solute of 60:1 is plotted with solid line and solute-water pair distribution with dashed. Functions are presented for the following directions: (a) 0° , (b) 30° , (c) 45° , and (d) 60° . LJ parameter for nonpolar molecules is $\sigma_{LJ}^{22} = 0.7r_{HB}$.

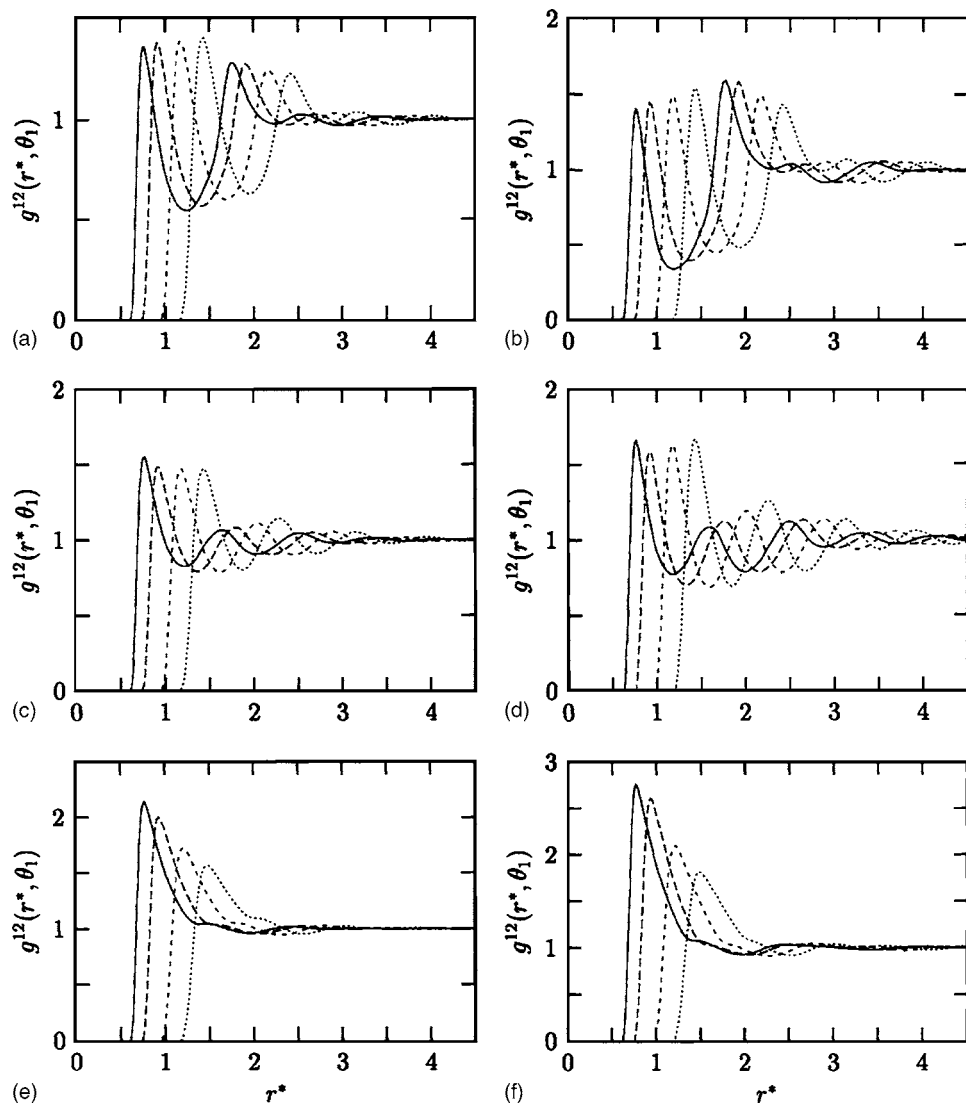


FIG. 7. Water-solute pair distribution, $g(r, \theta_1)$ for various orientations θ_1 of the water molecule, averaged over all possible θ_2 values for different temperatures and sizes of nonpolar molecules. Functions for $\sigma_{LJ}^{22} = 0.7r_{HB}$ are drawn by full line, $\sigma_{LJ}^{22} = 1.0r_{HB}$ with long-dashed line, $\sigma_{LJ}^{22} = 1.5r_{HB}$ with short-dashed, and $\sigma_{LJ}^{22} = 2.0r_{HB}$ dotted line. Functions are presented for the following θ_1 values and temperatures: (a) 0° , $T^* = 0.24$, (b) 0° , $T^* = 0.18$, (c) 30° , $T^* = 0.24$, (d) 30° , $T^* = 0.18$, (e) 60° , $T^* = 0.24$, and (f) 60° , $T^* = 0.18$.

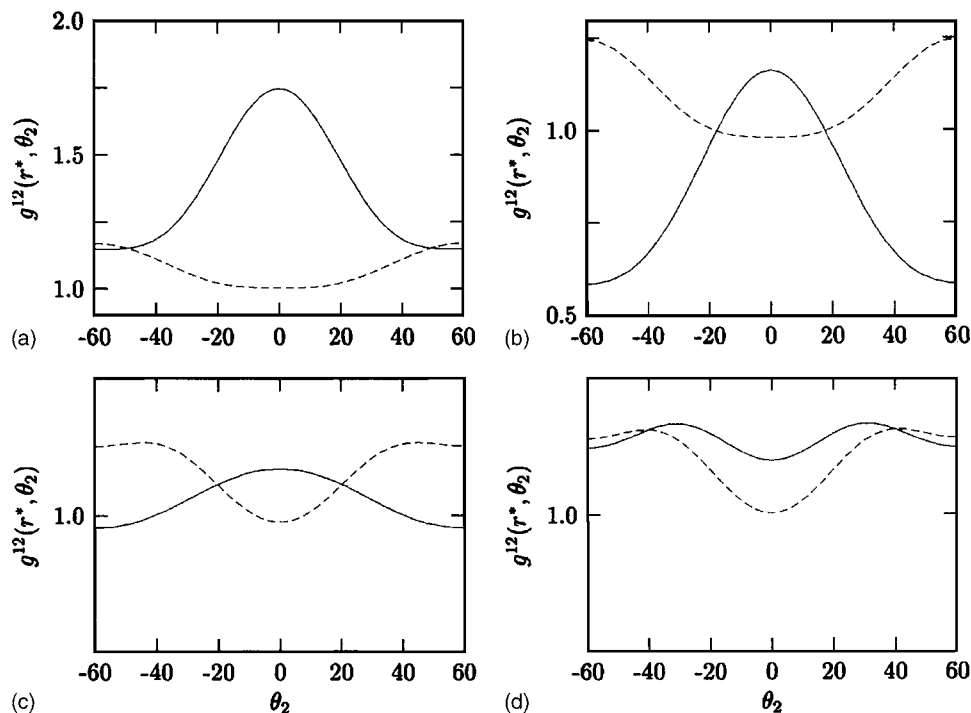


FIG. 8. Two-dimensional cuts through the solute-water distribution $g(r^*, \theta_1, \theta_2)$ as a function of θ_2 in first and second solvation shells around nonpolar solute of different sizes. Functions are presented for the following data: $T^* = 0.24$ and water density $\rho_1^* = 0.87$ and (a) $\sigma_{LJ}^{22} = 0.7r_{HB}$, $r_1^* = 0.7$, $r_2^* = 1.7$, (b) $\sigma_{LJ}^{22} = 1.0r_{HB}$, $r_1^* = 0.85$, $r_2^* = 1.85$, (c) $\sigma_{LJ}^{22} = 1.5r_{HB}$, $r_1^* = 1.1$, $r_2^* = 2.1$, and (d) $\sigma_{LJ}^{22} = 2.0r_{HB}$, $r_1^* = 1.35$, $r_2^* = 2.35$. Functions for waters in first solvation shell are drawn by solid line and for waters in second solvation shell by dashed lines.

is an improvement over the angle-averaged theory, we also find relatively poor agreement with the simulations for solute-solute correlation functions at low temperatures.

An advantage of the improved IET is that it yields the angular distributions of the model water molecules. In this section we compare our theory with the Monte Carlo results for the angular distributions of nonpolar solute around water. Figure 5 shows the coefficients of the expansion of the two-particle solute—water distribution function $g^{12}(r^*, \theta_1, \theta_2)$ for MB water molecules. We find that the IET follows the MC data quite well qualitatively. The size of nonpolar solute molecule is the same as the size of water: $\sigma_{LJ}^{22} = 0.7r_{HB}$, and the ratio between water density and density of nonpolar solute is 60:1. Agreement is much better at high temperatures.

Figure 6 shows the orientational distribution function for water molecules, at temperatures where ADIET predictions are good. Figure 6 shows $g^{12}(r^*, \theta_1)$ where the first molecule is fixed in orientation θ_1 , and we calculate the distributions with respect to r^* averaging over all θ_2 values ($g(r^*, \theta_1) = \langle g(r^*, \theta_1, \theta_2) \rangle_{\theta_2}$). The results for different directions given by angle θ_1 are shown in this figure ($0^\circ, 30^\circ, 45^\circ$ in 60°). Water-water distribution is presented by dashed line and solute-water distribution by solid at temperature $T^* = 0.24$ and density of water molecules $\rho_1^* = 0.87$. We find that nonpolar solutes are largely located in cavities in which waters can form water-water hydrogen bonds, but we also find broken hydrogen bonding, probably because the temperature is high for the results in this figure.

Figure 7 also gives distributions of water orientations, but now for solutes of different sizes, and at two different reduced temperatures: 0.24 and 0.18. We find that waters have orientational preferences around small solutes, but not around larger ones, consistent with other studies¹⁷ and with the view that large solutes force waters to break hydrogen bonds, so that there is no further advantage to any particular

orientation. The same conclusion follows from a study of water orientations in the first and second solvation shells around the nonpolar solute shown in Fig. 8.

V. CONCLUSIONS

We have developed theory for nonpolar solvation in water. Our goal here has been to extend the Wertheim theory of associated fluids^{23,24} to account for the coupled orientation dependence of interactions that arises from multiple hydrogen bonding arms within water molecules. As a simple test bed for developing the theory, we have used the well-understood and extensively simulated two-dimensional MB model of water. We have developed a multidensity OZ theory with explicit orientation dependence. We show that introduction of the orientation dependence yields better agreement with Monte Carlo computer simulations of the structural and thermodynamic properties than a simpler IET theory that averages over the angular orientations of waters.

The present theory has the virtue of making good qualitative predictions of the structural properties, with comparable insights into the properties of water, but with a gain in computational speed of about two orders of magnitude. Main advantage over orientationally averaged version is that here we can also study orientations of water molecules around solutes and not only the distance dependent structures. We believe that the reason why theory works only qualitatively for cold water is in the approximate closure used in IET. For better results bridge functions would have to be implemented, but they are not known for this model system.

ACKNOWLEDGMENTS

This work was supported by the Slovenian Research Agency (Physical Chemistry Research Program 0103-0201

and Research Project No. J1-6653) and by NIH grant GM063592.

- ¹D. Eisenberg and W. Kauzmann, *The Structure and Properties of Water* (Oxford University Press, Oxford, 1969).
- ²*Water, a Comprehensive Treatise*, edited by F. Franks (Plenum, New York, 1972) Vols. 1–7.
- ³F. H. Stillinger, *Science* **209**, 451 (1980).
- ⁴C. Tanford, *The Hydrophobic Effect: Formation of Micelles and Biological Membranes*, 2nd ed. (Wiley, New York, 1980).
- ⁵G. Robinson, S.-B. Zhu, S. Singh, and M. Evans, *Water in Biology, Chemistry and Physics: Experimental Overviews and Computational Methodologies* (World Scientific, Singapore, 1996).
- ⁶L. R. Pratt, *Annu. Rev. Phys. Chem.* **53**, 409 (2002).
- ⁷B. Widom, P. Bhimalapuram, and K. Koga, *Phys. Chem. Chem. Phys.* **5**, 3085 (2003).
- ⁸J. H. Griffith and H. A. Scheraga, *J. Mol. Struct.: THEOCHEM* **682**, 97 (2004).
- ⁹D. M. Huang and D. Chandler, *J. Phys. Chem. B* **106**, 2047 (2002).
- ¹⁰M. Predota, A. Ben-Naim, and I. Nezbeda, *J. Chem. Phys.* **118**, 6446 (2003).
- ¹¹I. Nezbeda, *J. Mol. Liq.* **73/74**, 317 (1997).
- ¹²D. E. Smith and A. D. J. Haymet, in *Reviews in Computational Chemistry*, edited by K. B. Lipkowitz, R. Larter, and T. R. Cundari (Wiley-VCH, New York, 2003).
- ¹³A. Ben-Naim, *J. Chem. Phys.* **54**, 3682 (1971).
- ¹⁴G. Andoloro and R. M. Sperandio-Mineo, *Eur. J. Phys.* **11**, 275 (1990).
- ¹⁵K. A. T. Silverstein, A. D. J. Haymet, and K. A. Dill, *J. Am. Chem. Soc.* **120**, 3166 (1998).
- ¹⁶K. A. T. Silverstein, K. A. Dill, and A. D. J. Haymet, *Fluid Phase Equilib.* **150-151**, 83 (1998).
- ¹⁷N. T. Southall and K. A. Dill, *J. Phys. Chem. B* **104**, 1326 (2000).
- ¹⁸K. A. T. Silverstein, K. A. Dill, and A. D. J. Haymet, *J. Chem. Phys.* **114**, 6303 (2001).
- ¹⁹B. Hribar Lee, N. T. Southall, V. Vlachy, and K. A. Dill, *J. Am. Chem. Soc.* **124**, 12302 (2002).
- ²⁰T. Urbic, V. Vlachy, and K. A. Dill, *J. Phys. Chem. B* **110**, 4963 (2006).
- ²¹T. Urbic, V. Vlachy, Yu. V. Kalyuzhnyi, N. T. Southall, and K. A. Dill, *J. Chem. Phys.* **112**, 2843 (2000).
- ²²T. Urbic, V. Vlachy, Yu. V. Kalyuzhnyi, N. T. Southall, and K. A. Dill, *J. Chem. Phys.* **116**, 723 (2002).
- ²³T. Urbic, V. Vlachy, Yu. V. Kalyuzhnyi, and K. A. Dill, *J. Chem. Phys.* **118**, 5516 (2003).
- ²⁴M. S. Wertheim, *J. Stat. Phys.* **42**, 477 (1986).
- ²⁵M. S. Wertheim, *J. Chem. Phys.* **87**, 7323 (1987).
- ²⁶E. V. Vakarín, Yu. Ja. Duda, and M. F. Holovko, *Mol. Phys.* **90**, 611 (1997).
- ²⁷L. Blum and A. J. Torruella, *J. Chem. Phys.* **56**, 303 (1972).
- ²⁸J. M. Caillol, D. Levesque, and J. J. Weis, *Mol. Phys.* **44**, 733 (1981).
- ²⁹D. A. Ward and F. Lado, *Mol. Phys.* **63**, 623 (1988).
- ³⁰D. A. Ward and F. Lado, *Mol. Phys.* **64**, 1185 (1988).
- ³¹J. Richardi, P. H. Fries, and H. Krienke, *J. Phys. Chem. B* **102**, 5196 (1998).
- ³²P. H. Fries and J. Richardi, *J. Chem. Phys.* **113**, 9169 (2000).
- ³³J. P. Hansen and I. R. McDonald, *Theory of Simple Liquids* (Academic, London, 1986).
- ³⁴S. W. Rick and A. D. J. Haymet, *J. Chem. Phys.* **90**, 1188 (1989).
- ³⁵J. D. Talman, *J. Comput. Phys.* **29**, 35 (1978).
- ³⁶K. A. T. Silverstein (unpublished).